Contents lists available at Science-Gate

International Journal of Advanced and Applied Sciences

Journal homepage: http://www.science-gate.com/IJAAS.html

Control of the free convective heat transfer using a U-shaped obstacle in an Al_2O_3-water nanofluid filled cubic cavity

Rajab Al-Sayagh *

Department of Mechanical Engineering, College of Engineering, Northern Border University, Arar, Saudi Arabia

ARTICLE INFO

Article history:
Received 13 December 2020
Received in revised form
26 February 2021
Accepted 15 March 2021

Keywords:
Nanofluid
Natural convection
U-shaped obstacle
3D

ABSTRACT

This paper deals with the study of free convection in a 3D enclosure filled with Al_2O_3-nanofluid and equipped with a U-shaped obstacle. The used U-shaped obstacle is considered perfectly conductive. The effect of the dimension and the orientation of the obstacle is investigated. In addition, the parameters governing the problem are varied as Rayleigh number (10^3 to 10^6), and nanoparticles volume fraction (0 to 7.5%). Results are depicted in terms of flow structures, temperature fields, and Nusselt number. Results show that the obstacle dimension and orientation can control the flow and optimize the heat transfer and the addition of nanoparticles enhances significantly Nusselt number.

1. Introduction

Natural convection is a mode of heat transfer that occurs in several engineering and industrial applications (Attia et al., 2021; Mahian et al., 2019; Kasaeian et al., 2017) such as electronic component cooling, geothermal engineering, renewable energies, HVAC, and thermal comfort in the building. The enhancement of heat transfer using non-destructive methods becomes a trend in the last decade. One of these methods comes from the use of nanofluids as an innovative technique. The nanofluids are suspensions of nanosized particles inside base fluids (water, oils, refrigerants…). Several studies related to this subject can be found in the literature.

Hussain et al. (2020) investigated the mixed convection of hybrid nanofluid in wavy channels having a fixed cylindrical obstacle. The proportions of Al_2O_3 and Cu nanoparticles are equitable. The authors indicated that the heat transfer is significatively affected by adding nanoparticles. Hassen et al. (2020) studied the electrohydrodynamic effect in addition to the use of an MWCTN-nanofluid in a square enclosure filled with a dielectric fluid. It was found that the combination of these non-destructive techniques allows a noticeable enhancement of the heat transfer. Almeshaal et al. (2020a) considered the aggregation effect on the Rayleigh-Bénard free convection in an L-shaped enclosure. The authors mentioned that the addition of the nanotubes influences the flow and temperature fields. Kolsi et al. (2020) studied the 3D MHD connection of CNT-nanofluid. It was found that the MHD effect opposes the nanofluid effect and reduces the heat transfer. Rashidi et al. (2020) studied the effect of nanofluid concentration on the irreversibility production in a cylindrical cavity subjected to various boundary conditions. It was found that the addition of nanoparticles can be used as an entropy generation optimizing parameter. Almeshaal et al. (2020b) studied the 3D free convection of hybrid Al_2O_3-CNT-nanofluid in a 3D T-shaped enclosure. The main results were that the use of the nanofluid leads to an intensification of the heat transfer and the viscous effects.

Kolsi et al. (2019) studied the 3D MHD thermocapillary convection of CNT-nanofluid. The authors concluded that the magnetic field opposes both the buoyancy and capillary forces. Complex boundary conditions were imposed in the work of Hussein et al. (2019) who considered the mixed convection of hybrid Gr-Pl nanofluid. They concluded that the addition of nanoparticles contributes to the apparition of more complex flow structures. Ahmed et al. (2019) investigated the effect of using an adiabatic obstacle on the mixed convective heat transfer of dispersed Cu in water by considering the effect of an external magnetic field. It was found that the obstacle and the magnetic effects collaborate in controlling the flow. Rahimi et al.

* Corresponding Author.
Email Address: rajab.alsayegh@nbu.edu.sa
https://doi.org/10.21833/ijaas.2021.07.004
Corresponding author's ORCID profile:
https://orcid.org/0000-0001-9940-9110

(2019) considered a multipipe enclosure containing Cu-nanofluid at various nanoparticle concentrations. The authors mentioned that the hydrothermal properties are very sensitive to the concentration of nanoparticles. Kolsi et al. (2019) considered a moving obstacle included in a 3D triangular closed domain containing Al_2O_3/water-nanofluid. They concluded that the combination of the moving fin and adding nanoparticles intensify the 3D character of the flow and lead to heat transfer intensification. Al-Rashed et al. (2019) considered a specific configuration corresponding to an open 3D parallelogrammic cavity partially heated and filled with a nanofluid. The results show that the dimension of the heater is the most important parameter affecting heat transfer. Al-Rashed et al. (2018a) studied the magnetoconvection of CNT-nanofluid. It was found that the inclination of the magnetic field is an optimizing parameter. A similar configuration was considered by Al-Rashed et al. (2018b) but by applying the magnetic field partially. The author mentioned that the intensity of flow is very affected by the magnetic field, especially in the active zone. Rahimi et al. (2018d) used the LBM technique to study entropy generation during nanofluid convection in a partially heated closed domain. The position and size of the partial active walls were found to significantly influence the flow, temperature field, and heat transfer. Other interesting papers in the field exist in the literature Rahimi et al. (2018a; 2018b; 2018c), Al-Rashed et al. (2017), Al-Sayegh (2018), Kasaeipoor et al. (2017), Rostami et al. (2020), Safaei et al. (2018), Akbari et al. (2016), Yousefzadeh et al. (2020), Pordanjani et al. (2019), Oztop and Abu-Nada (2008), Bondareva et al. (2017), Selimefendigil et al. (2016), and Kolsi et al. (2017a; 2017b).

According to the above-presented literature review and the author knowledge's, there no studies related to the use of a perfectly conductive U-shaped obstacle to control the convective heat transfer in cubic enclosures containing nanofluids. The originality of the paper consists of studying a 3D mathematical formulation based on the FEM. The various cases related to the orientation of the obstacle are considered and the effects of the Rayleigh number and the nanoparticles volume fraction are investigated. The structure of the present paper is as follows: An introduction presenting the recent works related to nanofluid convection, then the studied configuration, governing equations, and numerical method are detailed, after that the results will be described and discussed and finally a conclusion summarizes the main findings.

2. Mathematical formulation

The studied configuration consisting of a 3D differentially heated cubic enclosure filled with Al_2O_3/water-nanofluid and having and incorporated U-shaped obstacle is presented in Fig. 1a. The obstacle is considered perfectly conductive with fixed height (0.4L) and variable width (W). Four orientations of the obstacle were considered and named cases 1 to 4. Except for the active right and left walls, all the other walls are thermally insulated. Fig. 1b shows orientations of the U-shaped obstacle.

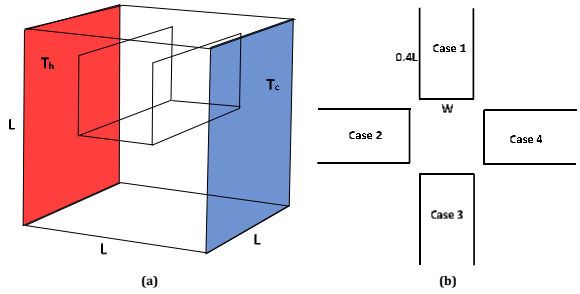

Fig. 1: (a) considered configuration; (b) Orientations of the U-shaped obstacle

After considering the following dimensionless variables:

$$t = \frac{t'}{L'^2/\alpha'};\ (X,Y,Z) = \frac{(X,Y,Y)'}{L'};\ \vec{U} = \frac{\vec{U}'}{\alpha_f/L'};\ P = \frac{P'}{\rho_f(\alpha_f/L')};\ \theta = \frac{T'-T_c'}{T_h'-T_c'}.$$

The governing equations become:

$$\vec{\nabla}.\vec{U} = 0 \quad (1)$$

$$\frac{\partial \vec{U}}{\partial t} + (\vec{U}.\vec{\nabla})\vec{U} = -\vec{\nabla}P + \Pr\left(\frac{\nu_{nf}}{\nu_f}\right)\Delta\vec{U} + \left(\frac{\beta_{nf}}{\beta_f}\right)Ra\Pr\vec{\theta}_g \quad (2)$$

$$\frac{\partial \theta}{\partial t} + \vec{U}.\nabla\theta = \frac{\alpha_{nf}}{\alpha_f}\nabla^2\theta \quad (3)$$

with

$$\Pr = \frac{\nu_f}{\alpha_f} \text{ and } Ra = \frac{\beta_f.g.L'^3.\Delta T}{\alpha_f\nu_f} \quad (4)$$

The local and average Nusselt numbers at the hot wall are:

$$Nu = \left(\frac{k_{nf}}{k_f}\right)\frac{\partial T}{\partial x}\Big|_{x=0} \text{ and } Nu_a = \frac{1}{L}\int_0^1\int_0^1 Nu\cdot dy\cdot dz \quad (5)$$

The following expressions are used to evaluate the thermophysical properties of the Al_2O_3-nanofluid (Kolsi et al., 2017a; 2017b):

$$\rho_{nf} = \phi\rho_{np} + (1-\phi)\rho_f \quad (6)$$

$$(\rho C_p)_{nf} = (1-\phi)(\rho C_p)_f + \phi(\rho C_p)_{np} \quad (7)$$

$$\frac{k_{nf}}{k_f} = \frac{k_{np}+2k_f-2\phi(k_f-k_{np})}{k_{np}+2k_f+\phi(k_f-k_{np})} \quad (8)$$

$$\mu_{nf} = \frac{\mu_f}{(1-\phi)^{2.5}}. \quad (9)$$

The properties of the nanoparticles and the base fluid are summarized in Table 1 (Kolsi et al., 2016).

The applied boundary conditions are:

- T = 1 at x = 0, T = 0 at x = 0, $\frac{\partial T}{\partial n} = 0$ on the remaining lateral, top, and bottom walls (10)
- $\vec{U} = \vec{0}$ on all the walls, (11)

The governing equations (Eqs. 1-3) are developed and solved based on the FEM method. The Galerkin weighted residual method is used and the variables are approximated via the Lagrange finite elements. More details on the used numerical method can be found in Al-Sayegh (2018).

3. Verification and mesh dependency test

The validation of the present numerical model is performed by comparing it with the flow structures presented in the work of Kolsi et al. (2016) (Fig. 2). The flow structures at the central plane for Ø=0.05 and Ra=10^5 and 10^6 show excellent conformity between the results. The results of the grid independence test are presented in Table 1. The Nusselt number was chosen as a sensitive variable. Four grids were tested (EN1 to EN4) the incremental increase between EN3 and EN4 is only 1.214%. Thus, for time economy and results accuracy the mesh number EN3 was retained for all the performed computations.

Table 1: Thermophysical properties of water and Al_2O_3 nanoparticle

property	Water	Al_2O_3
C_p (J/kg.K)	4179	765
ρ(kg/m^3)	997.1	3970
k (W/m.K)	0.613	40
βx 10^{-5} (1 /K)	21	0.85

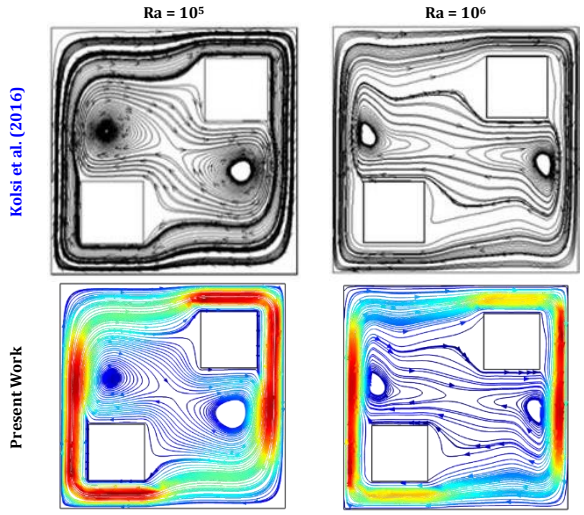

Fig. 2: Comparison of the flow structure in the central plane (z=0.5) with the results of Kolsi et al. (2016) for ϕ=0.15

Table 2: Mesh dependency test for case 2, Ra=10^6, W=0.08, and Ø=0.05.

Element Numbers	Nu_{avg}	% Increase	% Incremental increase
EN1:46746	10.718	-	-
EN2: 118916	10.985	2.491	-
EN3: 218454	11.199	4.487	1.948
EN4: 554270	11.335	5.756	1.214

4. Results and discussion

This section is dedicated to present and discuss the results of the numerical simulation performed to investigate the natural convection of Al_2O_3-nanofluid in a 3D cavity equipped with a U-shaped obstacle. Four cases related to the orientation of the obstacle are studied and the ranges of the considered parameters and variables are Rayleigh number (Ra) from 10^3 to 10^6, Al_2O_3 volume fraction (Ø) from 0 to 7.5%, and obstacle width (W) from 0.2 to 0.8.

Fig. 3 presents the 3D flow structures for the four considered cases at Ra=10^5 for W=0.2 and Ø=0 and 7.5%. The flow structure is very complex due to the 3D behavior of the configuration. The particle trajectories are not closed (in opposition with 2D configurations) and pass transversally through the cavity from a constant z-plan to another. The magnitude of the velocity is higher close to the right and left active walls. The minimum values of velocities occur in the region delimited by the U-shaped obstacle and cause a quasi-stagnant region where a small and slow recirculation vortex exists. For cases 1 and 3 the flow is characterized by two principal counter-rotative vortexes (under the obstacle for case 1 and on it for case 3). Higher nanoparticles concentrations cause an increase in the distance between these vortexes. For cases 2 and 4 only one principal clockwise circulation exists behind the closed part of the U-obstacle.

Fig. 4 illustrates the temperature fields for all the considered cases Ra=10^5 and W=0.2. The gray iso-surfaces correspond to ϕ =0 (pure water) and the colored iso-surfaces are for ϕ =0.075. The iso-surfaces of temperature are concentrated close to the top region of the cold wall and the lower region of the hot wall. At the core region, a vertical stratification occurs and becomes more important by adding the nanoparticles due to the enhancement of the heat transfer rate due to the increase of the

thermal conductivity. The presence of the obstacle causes a distortion of the isothermal surfaces due to the stagnant zone delimited by the obstacle.

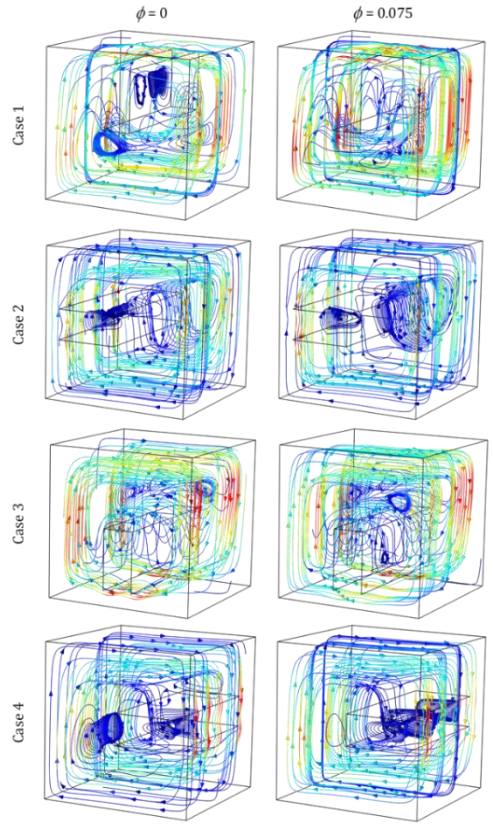

Fig. 3: 3D flow structure for the four considered cases and for Ra=10^5 and W=0.2

Since the flow structures present in Fig. 4 are very complex, and for a better understanding of the effected of the governing parameters on the particle trajectories behavior, Figs. 5 and 6 were plotted. Fig. 6 depicts the effect of the Rayleigh number on the flow structure at the central XY-plan for case 3 at ϕ =0 and 7.5%. The effect of Rayleigh number on the central flow structure is very clear, in fact for low Ra values it is characterized by a single principal recirculating vortex in addition to the secondary vortex occurring inside the obstacle. By increasing Ra values the principal vortex is dissociated into 2 vortexes.

The distance between these vortexes becomes more important as Ra increases. From Fig. 5, it can be also noticed that adding nanoparticles is more effective on the flow structure for higher Ra values. In fact, for Ra=10^3 the structures are quasi-similar. For Ra=10^4 the addition of nanoparticles causes the drifting of the principal vortexes to each other. For higher Ra values (Ra=10^6) an additional secondary clockwise recirculating vortex appears due to the viscous effects that cause higher shear stresses. It is also to be mentioned that the addition of nanoparticles, causes an intensification of the velocity magnitude due to the increase of the buoyancy forces.

As presented in Fig. 6, the flow structure is significantly affected by the orientation of the U-shaped obstacle. In Fig. 6, the width of the obstacle is W=0.2, this width is relatively thin thus for all the cases a fluid-stagnant region exists in the part delimited by the obstacle. It is also to be noticed that the higher velocity magnitudes occur for cases 2 and 4 due to strangulation caused by the obstacle close to the active walls. In fact, this strangulation causes a reduction of the flow section and thus higher velocities. The flow structure is more intense and more complex for Ra=10^6 compared to Ra=10^4. For cases 1 and 3, at Ra=10^4, only one principal vortex is encountered. For cases 2 and 4 an additional secondary vortex appears due to the vertical orientation of the obstacle that blocks the descending (or ascending) flow. For Ra=10^6, there are two clockwise co-rotative vortexes for cases 1 and 3, however, only one is encountered for cases 2 and 4.

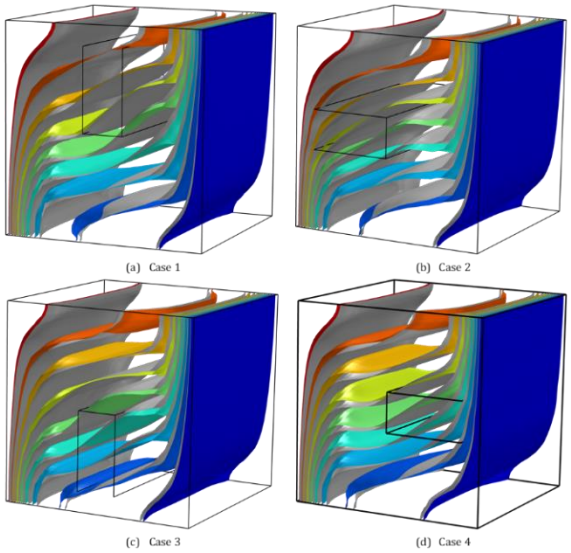

Fig. 4: 3D temperature field for the four considered cases and for Ra=10^5 and W=0.2; gray for (ϕ= 0) and colored for (ϕ= 0.075)

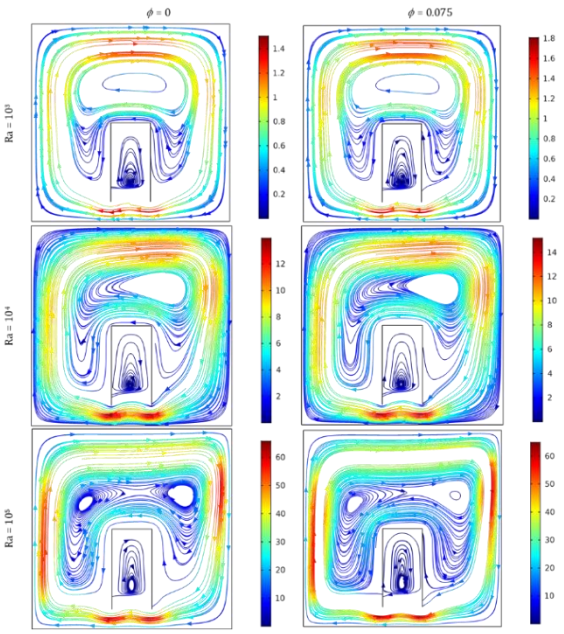

Fig. 5: Effect of Rayleigh number on flow structure at the central plan for case 3

The effect of the obstacle width on the flow structure is depicted in Fig. 7 for Ra=10^5 ϕ =5% while the width is varied from 0.2 to 0.8. The first ascertainment is that the flow structures are symmetric for cases 1 and 3 and for cases 2 and 4. The increase of the obstacle width causes a reduction of the size of the principal vortexes for cases 1 and 3 and the increase of the size of the secondary vortex existing inside the obstacle, this leads to a relative increase of the velocity magnitude in this region and reducing the stagnation zone. In opposition to cases 2 and 4, the principal vortex takes size by increasing the obstacle width. Concerning the velocity magnitude, it is noticed that higher values occur for cases 2 and 4.

Fig. 8 presents the effect of the obstacle width on the isotherms at the central plan for Ra=10^4 and 10^6. The black lines refer to ϕ =0 and the colored lines refer to ϕ =0.05. The presence of the obstacle causes the distortion of the isotherms passing through it. For Ra=10^6 a vertical stratification occurs at the central region of the enclosure and is more pronounced for ϕ =0.05 compared to ϕ =0. For low obstacle width's the isotherms are globally parallel indicating that in this region the conductive mode dominates the convection due to the stagnation of the fluid.

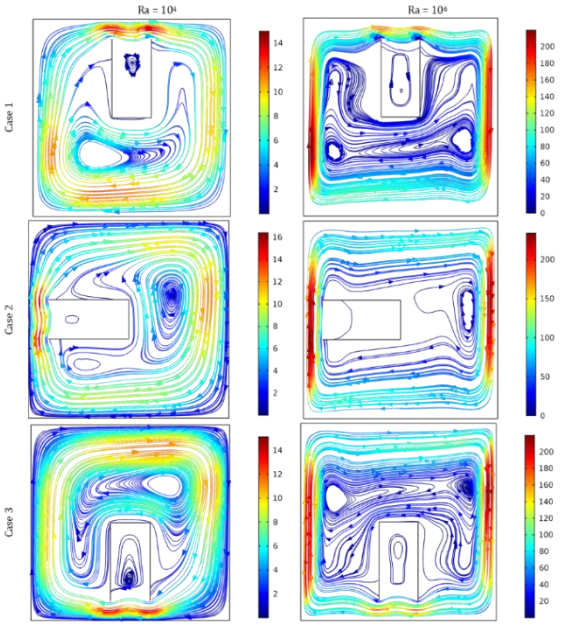

Fig. 6: Obstacle orientation effect on Flow structure at the central plan for Ra=10^4 and 10^6, W=0.2 and ϕ=0.05

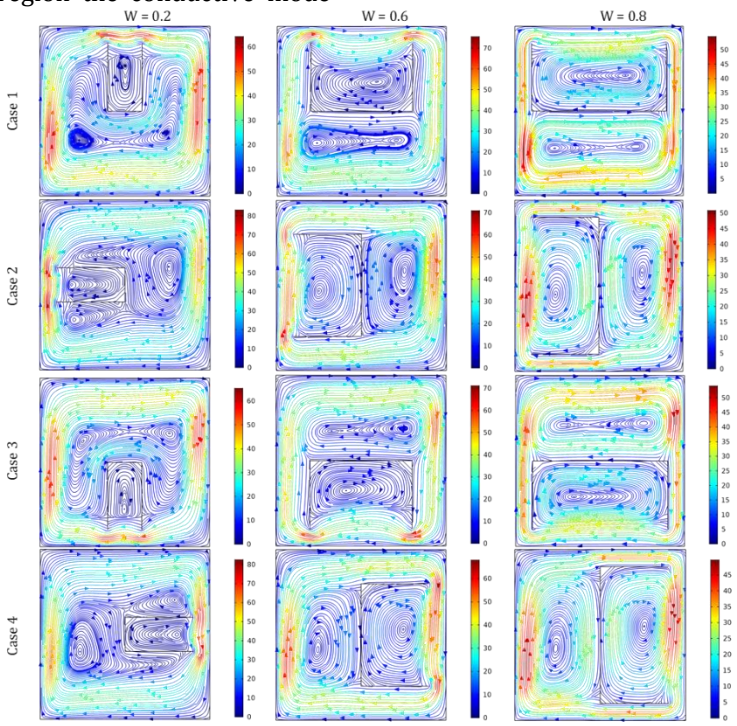

Fig. 7: Effect of the obstacle width on Flow structure at the central plan for Ra = 10^5 and ϕ=0.05

The effects of Rayleigh number and adding nanoparticles on the local Nusselt number are presented in Fig. 9. At fixed Rayleigh number the iso-lines of local Nusselt number are similar for pure water and nanofluid but their values are higher for nanofluid. The increasing of Rayleigh increases the local Nusselt number indicating a higher heat transfer. The iso-lines of the Nusselt number are horizontal at the central zone of the wall and curved close to the left and right edges. This behavior is more pronounced for high Ra values.

The effect of Al_2O_3 nanoparticles volume fraction on the heat transfer is studied by evaluating the average Nusselt number as presented in Fig. 10. For all the considered Rayleigh numbers, obstacle widths, and cases, the addition of the nanoparticles causes an enhancement of the heat transfer rate. The percentage of this increase is more important for low Ra values. As illustration for case 1 and W=0.2, the percentage of increase of Nu_{av} at ϕ =0.075 compared to the pure fluid (ϕ =0) is about 45% for Ra=10^4 and about 38.5% for Ra=10^6. This result is due to the increase of the viscous effects due to the higher velocity magnitudes for higher Ra.

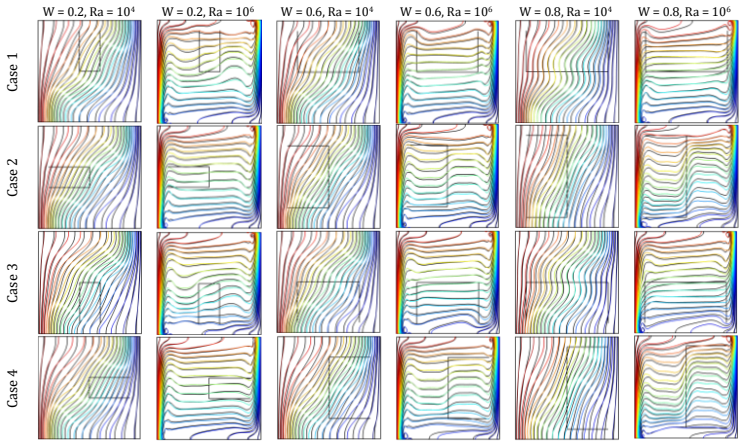

Fig. 8: Effect of the obstacle width on the isotherms at the central plan for Ra = 10^4 and 10^6; black lines for ϕ=0 and colored lines for ϕ=0.05

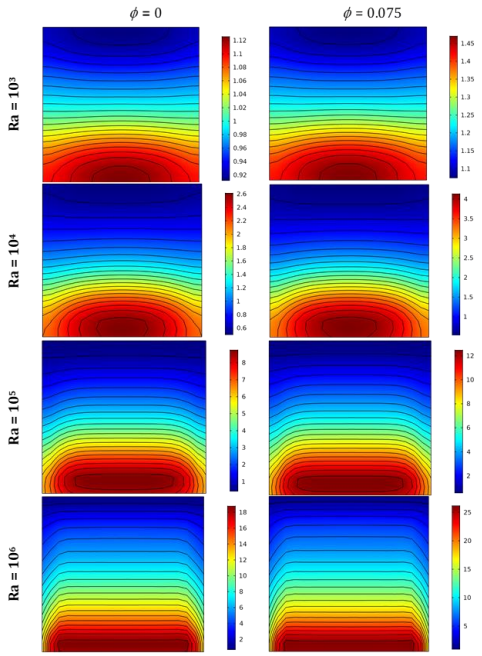

Fig. 9: Local Nusselt number at the left wall for case 1 and W = 0.2

The effect of the obstacle width on the average Nusselt number is depicted in Fig. 11 for ϕ =0.05. Fig. 11 shows that the optimization (minimization or maximization) of heat transfer can be essentially controlled by the obstacle width and orientation. Except for Ra=10^6, for all the other Ra values the maximum heat transfer rate occurs for W=0.2 and the minimum for W=0.8. The interesting result is that this variation not monotone for some configurations especially for case 2 where the heat transfer increases for W=0.6 and decreases again for W=0.8. For cases 1 and 3 at Ra=10^6, the variation of Nu_{av} is completely reversed and the minimum occurs at W=0.2 and the maximum at W=0.8.

5. Conclusion

In this paper, the 3D free convection of Al_2O_3/water-nanofluid in a cavity including a U-shaped obstacle is investigated numerically. The main findings can be summarized as follow:

- The flow structure is very complex, and the 3D character is more pronounced for higher Ra values and higher nanoparticle volume fractions.
- For high Ra values, the temperature field is characterized by a vertical thermal stratification that intensifies by adding the nanoparticles and is distorted by the presence of the obstacle.
- The increase of the obstacle width affects the flow structure by increasing the size of the principal recirculation vortexes and reducing the stagnation inside the obstacle.
- The width and the orientation of the obstacle can be used to optimize the heat transfer rate.

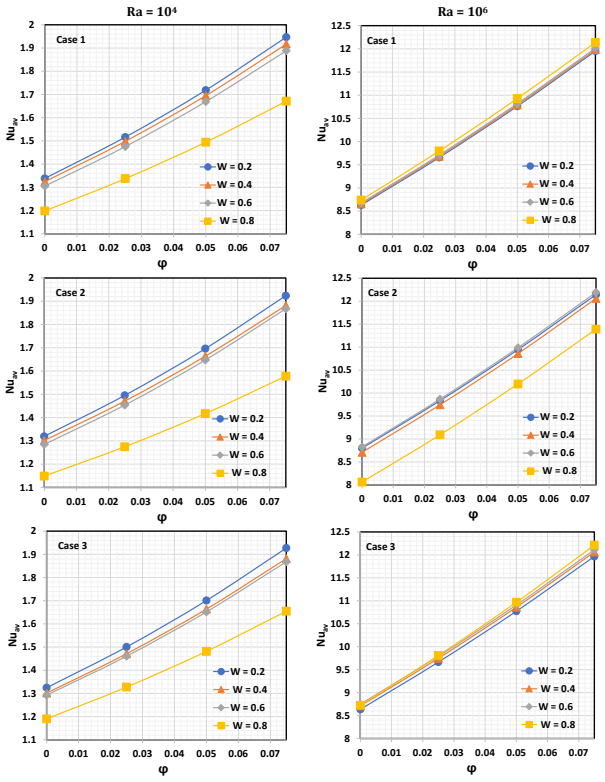

Fig. 10: Average Nusselt number versus the nanoparticle's concentration

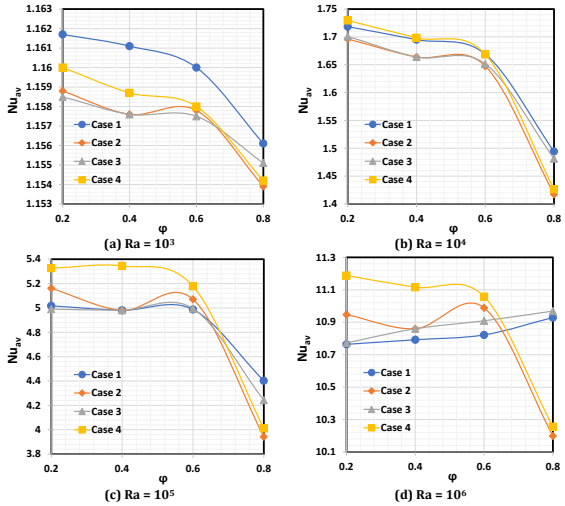

Fig. 11: Average Nusselt number versus the obstacle Width for ϕ=0.05 and various Rayleigh numbers

List of symbols

C_p	*Specific heat (J/kg. K)*
k	*Thermal conductivity (W/m.K)*
L	*Cavity width (m)*
Nu	*Nusselt number*
Pr	*Prandtl number*
Ra	*Rayleigh number*
t	*Dimensionless time*
T	*Dimensionless temperature*
$\vec{U}$	*Dimensionless velocity vector*
β	*Thermal expansion coefficient (1/ K)*
ρ	*Density (kg/m³)*
μ	*Dynamic viscosity (kg./m.s)*
ϕ	*Nanoparticles volume fraction*
av	*Average*
c	*cold*
f	*fluid*
h	*hot*
np	*nanoparticles*
nf	*nanofluid*
CNT	*Carbone-nanoTube*
FEM	*Finite Element Method*
MHD	*Magneto-hydrodynamics*

Compliance with ethical standards

Conflict of interest

The author(s) declared no potential conflicts of interest with respect to the research, authorship, and/or publication of this article.

References

Ahmed SE, Mansour MA, Hussein AK, Mallikarjuna B, Almeshaal MA, and Kolsi L (2019). MHD mixed convection in an inclined cavity containing adiabatic obstacle and filled with Cu–water nanofluid in the presence of the heat generation and partial slip. Journal of Thermal Analysis and Calorimetry, 138(2): 1443-1460. https://doi.org/10.1007/s10973-019-08340-3

Akbari OA, Safaei MR, Goodarzi M, Akbar NS, Zarringhalam M, Shabani GAS, and Dahari M (2016). A modified two-phase mixture model of nanofluid flow and heat transfer in a 3-D curved microtube. Advanced Powder Technology, 27(5): 2175-2185. https://doi.org/10.1016/j.apt.2016.08.002

Almeshaal MA, Kalidasan K, Askri F, Velkennedy R, Alsagri AS, and Kolsi L (2020b). Three-dimensional analysis on natural convection inside a T-shaped cavity with water-based CNT–aluminum oxide hybrid nanofluid. Journal of Thermal Analysis and Calorimetry, 139(3): 2089-2098 . https://doi.org/10.1007/s10973-019-08533-w

Almeshaal MA, Maatki C, Kolsi L, Ghachem K, and Chamkha A (2020a). 3D Rayleigh-Bénard-type natural convection in MWCNT-nanofluid-filled L-shaped enclosures with consideration of aggregation effect. Mathematical Methods in the Applied Sciences, 2020: 1-17. https://doi.org/10.1002/mma.6409

Al-Rashed AA, Kalidasan K, Kolsi L, Aydi A, Malekshah EH, Hussein AK, and Kanna PR (2018b). Three-dimensional investigation of the effects of external magnetic field inclination on laminar natural convection heat transfer in CNT–water nanofluid filled cavity. Journal of Molecular Liquids, 252: 454-468. https://doi.org/10.1016/j.molliq.2018.01.006

Al-Rashed AA, Kolsi L, Kalidasan K, Malekshah EH, Borjini MN, and Kanna PR (2017). Second law analysis of natural convection in a CNT-water nanofluid filled inclined 3D cavity with incorporated Ahmed body. International Journal of Mechanical Sciences, 130: 399-415. https://doi.org/10.1016/j.ijmecsci.2017.06.028

Al-Rashed AA, Kolsi L, Oztop HF, Aydi A, Malekshah EH, Abu-Hamdeh N, and Borjini MN (2018a). 3D magneto-convective heat transfer in CNT-nanofluid filled cavity under partially active magnetic field. Physica E: Low-Dimensional Systems and Nanostructures, 99: 294-303. https://doi.org/10.1016/j.physe.2018.02.011

Al-Rashed AAA, Hassen W, Kolsi L, Oztop HF, Chamkha AJ, and Abu-Hamdeh N (2019). Three-dimensional analysis of natural convection in nanofluid-filled parallelogrammic enclosure opened from top and heated with square heater. Journal of Central South University, 26(5): 1077-1088. https://doi.org/10.1007/s11771-019-4072-0

Al-Sayegh R (2018). Influence of external magnetic field inclination on three-dimensional buoyancy-driven convection in an open trapezoidal cavity filled with CNT-Water nanofluid. International Journal of Mechanical Sciences, 148: 756-765. https://doi.org/10.1016/j.ijmecsci.2018.09.032

Attia MEH, Hussein AK, Rout SK, Soli J, Elaloui E, Driss Z, and Chand R (2021). Experimental study of the effect of Al_2O_3 nanoparticles on the profitability of a single-slope solar still: Application in southeast of Algeria. In: Ramgopal M, Rout SK, Sarangi SK (Eds.), Advances in air conditioning and refrigeration: 119-133. Springer, Singapore, Singapore. https://doi.org/10.1007/978-981-15-6360-7_12

Bondareva NS, Sheremet MA, Oztop HF, and Abu-Hamdeh N (2017). Heatline visualization of natural convection in a thick walled open cavity filled with a nanofluid. International Journal of Heat and Mass Transfer, 109: 175-186. https://doi.org/10.1016/j.ijheatmasstransfer.2017.01.124

Hassen W, Kolsi L, Mohammed HA, Ghachem K, Sheikholeslami M, and Almeshaal MA (2020). Transient electrohydrodynamic convective flow and heat transfer of MWCNT-dielectric nanofluid in a heated enclosure. Physics Letters A, 384(28): 126736. https://doi.org/10.1016/j.physleta.2020.126736

Hussain S, Jamal M, Maatki C, Ghachem K, and Kolsi L (2020). MHD mixed convection of Al_2O_3–Cu–water hybrid nanofluid in a wavy channel with incorporated fixed cylinder. Journal of Thermal Analysis and Calorimetry, 1-15. https://doi.org/10.1007/s10973-020-10260-6

Hussein AK, Kolsi L, Almeshaal MA, Li D, Ali HM, and Ahmed IS (2019). Mixed convection in a cubical cavity with active lateral walls and filled with hybrid graphene–platinum nanofluid. Journal of Thermal Science and Engineering Applications, 11(4): 041007. https://doi.org/10.1115/1.4043758

Kasaeian A, Daneshazarian R, Mahian O, Kolsi L, Chamkha AJ, Wongwises S, and Pop I (2017). Nanofluid flow and heat transfer in porous media: A review of the latest developments.

International Journal of Heat and Mass Transfer, 107: 778-791. https://doi.org/10.1016/j.ijheatmasstransfer.2016.11.074

Kasaeipoor A, Malekshah EH, and Kolsi L (2017). Free convection heat transfer and entropy generation analysis of MWCNT-MgO (15%–85%)/Water nanofluid using Lattice Boltzmann method in cavity with refrigerant solid body-Experimental thermo-physical properties. Powder Technology, 322: 9-23. https://doi.org/10.1016/j.powtec.2017.08.061

Kolsi L, Algarni S, Mohammed HA, Hassen W, Lajnef E, Aich W, and Almeshaal MA (2020). 3D magneto-buoyancy-thermocapillary convection of CNT-water nanofluid in the presence of a magnetic field. Processes, 8(3): 258. https://doi.org/10.3390/pr8030258

Kolsi L, Alrashed AA, Al-Salem K, Oztop HF, and Borjini MN (2017b). Control of natural convection via inclined plate of CNT-water nanofluid in an open sided cubical enclosure under magnetic field. International Journal of Heat and Mass Transfer, 111: 1007-1018. https://doi.org/10.1016/j.ijheatmasstransfer.2017.04.069

Kolsi L, Kalidasan K, Alghamdi A, Borjini MN, and Kanna PR (2016). Natural convection and entropy generation in a cubical cavity with twin adiabatic blocks filled by aluminum oxide–water nanofluid. Numerical Heat Transfer, Part A: Applications, 70(3): 242-259. https://doi.org/10.1080/10407782.2016.1173478

Kolsi L, Lajnef E, Aich W, Alghamdi A, Aichouni MA, Borjini MN, and Aissia HB (2017a). Numerical investigation of combined buoyancy-thermocapillary convection and entropy generation in 3D cavity filled with Al_2O_3 nanofluid. Alexandria Engineering Journal, 56(1): 71-79. https://doi.org/10.1016/j.aej.2016.09.005

Kolsi L, Öztop HF, Al-Rashed AA, Aydi A, Naceur BM, and Abu-Hamdeh N (2019). Control of heat transfer and fluid flow via a moving fin in a triangular enclosure filled with nanofluid. Heat Transfer Research, 50(2): 159-181. https://doi.org/10.1615/HeatTransRes.2018019485

Mahian O, Kolsi L, Amani M, Estellé P, Ahmadi G, Kleinstreuer C and Pop I (2019). Recent advances in modeling and simulation of nanofluid flows-part II: Applications. Physics Reports, 791: 1-59. https://doi.org/10.1016/j.physrep.2018.11.003

Oztop HF and Abu-Nada E (2008). Numerical study of natural convection in partially heated rectangular enclosures filled with nanofluids. International Journal of Heat and Fluid Flow, 29(5): 1326-1336. https://doi.org/10.1016/j.ijheatfluidflow.2008.04.009

Pordanjani AH, Aghakhani S, Karimipour A, Afrand M, and Goodarzi M (2019). Investigation of free convection heat transfer and entropy generation of nanofluid flow inside a cavity affected by magnetic field and thermal radiation. Journal of Thermal Analysis and Calorimetry, 137(3): 997-1019. https://doi.org/10.1007/s10973-018-7982-4

Rahimi A, Azarikhah P, Kasaeipoor A, Malekshah EH, and Kolsi L (2019). Lattice Boltzmann simulation of free convection's hydrothermal aspects in a finned/multi-pipe cavity filled with CuO-water nanofluid. International Journal of Numerical Methods for Heat and Fluid Flow, 29(3): 1058-1078. https://doi.org/10.1108/HFF-07-2018-0349

Rahimi A, Kasaeipoor A, Amiri A, Doranehgard MH, Malekshah EH, and Kolsi L (2018a). Lattice Boltzmann method based on Dual-MRT model for three-dimensional natural convection and entropy generation in CuO–water nanofluid filled cuboid enclosure included with discrete active walls. Computers and Mathematics with Applications, 75(5): 1795-1813. https://doi.org/10.1016/j.camwa.2017.11.037

Rahimi A, Kasaeipoor A, Malekshah EH, and Kolsi L (2018d). Lattice Boltzmann simulation of free convection in nanofluid filled cavity with partially active walls–entropy generation and heatline visualization. International Journal of Numerical Methods for Heat and Fluid Flow, 28(10): 2254-2283. https://doi.org/10.1108/HFF-06-2017-0229

Rahimi A, Kasaeipoor A, Malekshah EH, Palizian M, and Kolsi L (2018b). Lattice Boltzmann numerical method for natural convection and entropy generation in cavity with refrigerant rigid body filled with DWCNTs-water nanofluid-experimental thermo-physical properties. Thermal Science and Engineering Progress, 5: 372-387. https://doi.org/10.1016/j.tsep.2018.01.005

Rahimi A, Sepehr M, Lariche MJ, Kasaeipoor A, Malekshah EH, and Kolsi L (2018c). Entropy generation analysis and heatline visualization of free convection in nanofluid (KKL model-based)-filled cavity including internal active fins using lattice Boltzmann method. Computers and Mathematics with Applications, 75(5): 1814-1830. https://doi.org/10.1016/j.camwa.2017.12.008

Rashidi I, Kolsi L, Ahmadi G, Mahian O, Wongwises S, and Abu-Nada E (2020). Three-dimensional modelling of natural convection and entropy generation in a vertical cylinder under heterogeneous heat flux using nanofluids. International Journal of Numerical Methods for Heat and Fluid Flow, 30(1): 119-142. https://doi.org/10.1108/HFF-12-2018-0731

Rostami S, Aghakhani S, Hajatzadeh Pordanjani A, Afrand M, Cheraghian G, Oztop HF, and Shadloo MS (2020). A review on the control parameters of natural convection in different shaped cavities with and without nanofluid. Processes, 8(9): 1011. https://doi.org/10.3390/pr8091011

Safaei MR, Karimipour A, Abdollahi A, and Nguyen TK (2018). The investigation of thermal radiation and free convection heat transfer mechanisms of nanofluid inside a shallow cavity by lattice Boltzmann method. Physica A: Statistical Mechanics and Its Applications, 509: 515-535. https://doi.org/10.1016/j.physa.2018.06.034

Selimefendigil F, Öztop HF, and Abu-Hamdeh N (2016). Mixed convection due to rotating cylinder in an internally heated and flexible walled cavity filled with SiO2–water nanofluids: Effect of nanoparticle shape. International Communications in Heat and Mass Transfer, 71: 9-19. https://doi.org/10.1016/j.icheatmasstransfer.2015.12.007

Yousefzadeh S, Rajabi H, Ghajari N, Sarafraz MM, Akbari OA, and Goodarzi M (2020). Numerical investigation of mixed convection heat transfer behavior of nanofluid in a cavity with different heat transfer areas. Journal of Thermal Analysis and Calorimetry, 140(6): 2779-2803. https://doi.org/10.1007/s10973-019-09018-6